Article

De Novo Design of a *D*-Symmetrical Protein that Reproduces the Diheme Four-Helix Bundle in Cytochrome *bc*

Giovanna Ghirlanda, Artur Osyczka, Weixia Liu, Michael Antolovich, Kevin M. Smith, P. Leslie Dutton, A. Joshua Wand, and William F. DeGrado

J. Am. Chem. Soc., **2004**, 126 (26), 8141-8147• DOI: 10.1021/ja039935g • Publication Date (Web): 15 June 2004

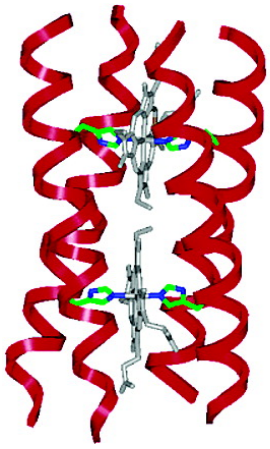

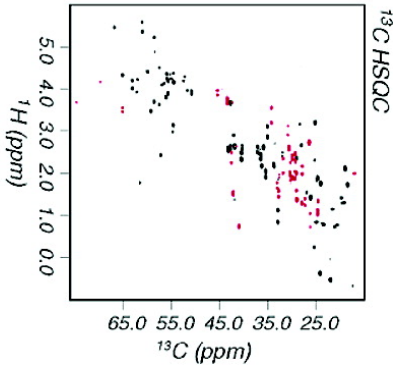

More About This Article

Additional resources and features associated with this article are available within the HTML version:

- Supporting Information
- Links to the 4 articles that cite this article, as of the time of this article download
- Access to high resolution figures
- Links to articles and content related to this article
- Copyright permission to reproduce figures and/or text from this article

View the Full Text HTML

J|A|C|S
ARTICLES
Published on Web 06/15/2004

De Novo Design of a D_2-Symmetrical Protein that Reproduces the Diheme Four-Helix Bundle in Cytochrome bc_1

Giovanna Ghirlanda,*[,†,‡] Artur Osyczka,[†] Weixia Liu,[†] Michael Antolovich,[||] Kevin M. Smith,[||] P. Leslie Dutton,[†] A. Joshua Wand,[†] and William F. DeGrado*[,†,§]

Contribution from The Johnson Research Foundation and Department of Biochemistry and Biophysics, University of Pennsylvania, Philadelphia Pennsylvania 19104; the Department of Chemistry and Biochemistry, Arizona State University, Tempe, Arizona 85287; the Department of Chemistry, University of Pennsylvania, Philadelphia, Pennsylvania 19104; and the Department of Chemistry, Louisiana State University, Baton Rouge, Louisiana 70803

Received December 3, 2003; E-mail: gghirlanda@asu.edu; wdegrado@mail.med.upenn.edu

Abstract: An idealized, water-soluble D_2-symmetric diheme protein is constructed based on a mathematical parametrization of the backbone coordinates of the transmembrane diheme four-helix bundle in cytochrome bc_1. Each heme is coordinated by two His residues from diagonally apposed helices. In the model, the imidazole rings of the His ligands are held in a somewhat unusual perpendicular orientation as found in cytochrome bc_1, which is maintained by a second-shell hydrogen bond to a Thr side chain on a neighboring helix. The resulting peptide is unfolded in the apo state but assembles cooperatively upon binding to heme into a well-folded tetramer. Each tetramer binds two hemes with high affinity at low micromolar concentrations. The equilibrium reduction midpoint potential varies between −76 mV and −124 mV vs SHE in the reducing and oxidizing direction, respectively. The EPR spectrum of the ferric complex indicates the presence of a low-spin species, with a g_{max} value of 3.35 comparable to those obtained for hemes *b* of cytochrome bc_1 (3.79 and 3.44). This provides strong support for the designed perpendicular orientation of the imidazole ligands. Moreover, NMR spectra show that the protein exists in solution in a unique conformation and is amenable to structural studies. This protein may provide a useful scaffold for determining how second-shell ligands affect the redox potential of the heme cofactor.

Introduction

The *de novo* design of heme proteins has proven to be a successful approach for understanding how the protein matrix influences the electrochemical midpoint and proton coupling of the bound cofactor. Two distinct approaches have been explored for this endeavor; Benson,[1,2] Lombardi and Pavone,[3−5] Suslick,[6,7] Mihara,[8,9] and their co-workers have focused on relatively simple models in which the heme is ensconced between two helical peptides, similar to a two-helix version of microperoxidase,[10] and more recently on heme-binding three-helix bundle models.[11] A second class of heme proteins involve a four-helix bundle,[12−22] which can bind between one and four heme moieties, depending on the design. Initial attempts to design heme proteins[14,17] were initiated prior to the development of modern computational methods for backbone[23−26] and side

† The Johnson Research Foundation and Department of Biochemistry and Biophysics, University of Pennsylvania.
‡ Arizona State University.
§ Department of Chemistry, University of Pennsylvania.
|| Louisiana State University.

(1) Benson, D. R.; Hart, B. R.; Zhou, X.; Doughty, M. B. *J. Am. Chem. Soc.* **1995**, *117*, 8502.
(2) Liu, D. L.; Williamson, D. A.; Kennedy, M. L.; Williams, T. D.; Morton, M. M.; Benson, D. R. *J. Am. Chem. Soc.* **1999**, *121*, 11798.
(3) D'Auria, G.; Maglio, O.; Nastri, F.; Lombardi, A.; Mazzeo, M.; Morelli, G.; Paolillo, L.; Pedone, C.; Pavone, V. *Chem.—Eur. J.* **1997**, *3*, 350−362.
(4) Nastri, F.; Lombardi, A.; Morelli, G.; Maglio, O.; DAuria, G.; Pedone, C.; Pavone, V. *Chem.—Eur. J.* **1997**, *3*, 340−349.
(5) Lombardi, A.; Nastri, F.; Sanseverino, M.; Maglio, O.; Pedone, C.; Pavone, V. *Inorg. Chim. Acta* **1998**, *276*, 301−313.
(6) Huffman, D. L.; Suslick, K. S. *Inorg. Chem.* **2000**, *39*, 5418−5419.
(7) Rosenblatt, M. M.; Huffman, D. L.; Wang, X.; Remmer, H. A.; Suslick, K. S. *J. Am. Chem. Soc.* **2002**, *124*, 12394−12395.
(8) Sakamoto, S.; Ueno, A.; Mihara, H. *J. Chem. Soc., Perkin Trans. 2* **1998**, 2395−2404.
(9) Sakamoto, S.; Obataya, I.; Ueno, A.; Mihara, H. *J. Chem. Soc., Perkin Trans 2* **1999**, 2059−2069.
(10) Aron, J.; Baldwin, D. A.; Marques, H. M.; Pratt, J. M.; Adams, P. A. *J. Inorg. Biochem.* **1986**, *27*, 227−243.
(11) Obataya, I.; Kotaki, T.; Sakamoto, S.; Ueno, A.; Mihara, H. *Bioorg. Med. Chem. Lett.* **2000**, *10*, 2719−2722.
(12) Rojas, N. R.; Kamtekar, S.; Simons, C. T.; McLean, J. E.; Vogel, K. M.; Spiro, T. G.; Farid, R. S.; Hecht, M. H. *Protein Sci.* **1997**, *6*, 2512−2524.
(13) Moffet, D. A.; Hecht, M. H. *Chem. Rev.* **2001**, *101*, 3191−3203.
(14) Robertson, D. E.; Farid, R. S.; Moser, C. C.; Urbauer, J. L.; Mulholland, S. E.; Pidikiti, R.; Lear, J. D.; Wand, A. J.; DeGrado, W. F.; Dutton, P. L. *Nature* **1994**, *368*, 425−432.
(15) Shifman, J. M.; Gibney, B. R.; Sharp, R. E.; Dutton, P. L. *Biochemistry* **2000**, *39*, 14813−14821.
(16) Gibney, B. R.; Huang, S. S.; Skalicky, J. J.; Fuentes, E. J.; Wand, A. J.; Dutton, P. L. *Biochemistry* **2001**, *40*, 10550−10561.
(17) Choma, C.; Lear, J. D.; Nelson, M. J.; Dutton, P. L.; Robertson, D. E.; DeGrado, W. F. *J. Am. Chem. Soc.* **1994**, *116*, 856−865.
(18) Rau, H. K.; Haehnel, W. *J. Am. Chem. Soc.* **1998**, *120*, 468−476.
(19) Rau, H. K.; DeJonge, N.; Haehnel, W. *Angew Chem., Int. Ed.* **2000**, *39*, 250−253.
(20) Fahnenschmidt, M.; Bittl, R.; Schlodder, E.; Haehnel, W.; Lubitz, W. *Phys. Chem. Chem. Phys.* **2001**, *3*, 4082−4090.
(21) Wei, Y.; Kim, S.; Fela, D.; Baum, J.; Hecht, M. H. *Proc. Natl. Acad. Sci. U.S.A.* **2003**.
(22) Wilson, J. R.; Caruana, D. J.; Gilardi, G. *Chem. Commun. (Camb)* **2003**, 356−357.
(23) Dahiyat, B. I.; Mayo, S. L. *Science* **1997**, *278*, 82−87.
(24) Desjarlais, J. R.; Handel, T. M. *J. Mol. Biol.* **1999**, *290*, 305−318.
(25) Harbury, P. B.; Plecs, J. J.; Tidor, B.; Alber, T.; Kim, P. S. *Science* **1998**, *282*, 1462−1467.

chain optimization.[24,27,28] Thus, many early proteins were highly dynamic, showing some of the properties of the molten globule. Subsequently, the hydrophobic side chains of an early designed protein were systematically varied, ultimately resulting in a peptide that was well structured in the apo state.[29,30] Similar experimental approaches allowed the definition of a protein that is better ordered in the presence of heme,[16] and more recently in a peptide that appears to be amenable to structural studies.[31]

Much of the early work on proteins had been aimed at reproducing the biophysical properties of cytochrome bc_1, which in the intervening years has been crystallographically characterized.[32−35] As expected from early models, the b subunit of cytochrome bc_1 shows a transmembrane four-helix bundle that binds two bis-His ligated hemes (b_L and b_H), which are essential for transferring electrons across the membrane between the two catalytic quinone binding sites. Even the detailed arrangement of the two His ligands, in an unusual orthogonal arrangement, was predicted by early EPR studies.[36] In an elegant series of papers, Haehnel, Lubitz, and their co-workers[18−20,37,38] have designed template-assembled peptide models for cytochrome *b*, in which two copies each of two different peptides were attached to a peptide framework. The peptides reproduce many of the properties of the hemes *b* sites in cytochrome bc_1. However, the heme appears to be in a heterogeneous environment in these models[20] which prompted us to examine whether some recently developed approaches to protein design[39] might result in a more homogeneous and uniquely structured site. Here, we use a mathematical parametrization of the backbone[26] of the essential region of the b subunit of cytochrome bc_1 as a starting point for the design of a water-soluble model for this protein. The designed peptide successfully recapitulates the essential spectroscopic and electrochemical properties of the two-heme b subunit of cytochrome bc_1.

Results

Design of a Symmetrical Two-Heme Bundle: The crystal structure of cytochrome bc_1 reveals a pair of bis-His ligated hemes residing within a central four-helix bundle formed by the b subunit. This helical bundle has *quasi* 2-fold symmetry with a helical pair as the asymmetric unit.[32,33] The two heme binding sites are highly similar. The two critical histidine residues are located on diagonally opposed helices, and their ϵ-nitrogens bind to the heme iron. The other two helices serve to shield the heme, and each has a conserved Gly residue allowing close contact with the heme. Finally, a conserved Thr side chain from the heme-shielding helix forms a second-shell hydrogen bond to the δ-nitrogen of the His side chain, possibly further constraining the orientation and electronic properties of this side chain.

The structure of the bc_1 bundle shows approximate two-fold symmetry with two sequentially distinct helices in the asymmetric unit; one of the helices in the asymmetric unit contains two of the essential His residues, while the other helix contains the conserved Gly and Thr residues. These essential amino acids are spaced by 14 residues, leading to two binding sites that are translated by 20 Å down the central axis of the bundle.

Previously, we demonstrated that the backbone conformation of the diheme-binding four-helix bundle in the b subunit of cytochrome bc_1 can be described to within 1 Å rmsd, using a mathematical model for a symmetrical antiparallel four-stranded coiled coil.[26] The coiled coil model has exact seven-residue periodicity, and the residues are designated "a" through "g" in the usual manner. The "*a*" and "*d*" positions are geometrically distinct and project toward the interior of the bundle. These "*a*" and "*d*" positions segregate into distinct layers, with two "*a*" and two "*d*" positions in each layer. In cytochrome bc_1, the Gly residue occurs at an "*a*" position and the His at a "*d*" position within the same layer.

While the diheme-binding four-helix bundle of cytochrome bc_1 structure has two copies each of two distinct helices (designated the heme-ligating and the heme-shielding helices by Fahnenschmidt et al.[20]), it appeared to us that one could design a D_2-symmetrical bc_1-like bundle by simply including the critical residues within a single helix. Thus, a His residue would be placed at a "*d*" position in the N-terminal heptad of the coiled coil, and the critical Gly would be placed at an "*a*" position at the C-terminal heptad. A Thr residue, immediately preceding the Gly in the sequence, is geometrically well positioned to accept a second-shell hydrogen bond from the His side chain. The number of intervening heptads would define the spacing of the hemes.

Indeed, a computational model built on this principle, shown in Figure 1a (see Materials and Methods), allowed the critical residues to be placed in appropriate geometries to recapitulate the geometry of the individual heme *b* binding sites in cytochrome bc_1: the critical His and Gly residues are positioned within the same layers, and the Thr residue is poised to hydrogen bond the δ nitrogen of the histidine (Figure 1b). With one intervening heptad, the hemes are spaced more closely than in cytochrome bc_1, with 14 Å between the heme irons. The hemes were positioned with their propionate groups pointing toward the extremities of the bundle; by analogy to cytochrome bc_1, two arginines were introduced in the first heptad to permit interaction with the negative charges. The space available to the side chains at the remaining "*a*" and "*d*" positions is generally highly restricted and was manually selected by examination of all hydrophobic amino acids in all possible low-energy rotamers to find an optimal fit with the steric requirements of the cavity. Because of the symmetry and geometric restrictions, there were very few possibilities for each residue. In the native protein, residues in positions "*b*", "*c*", and "*f*" are exposed to the protein matrix; in our model, these residues will

(26) North, B.; Summa, C. M.; Ghirlanda, G.; DeGrado, W. F. *J. Mol. Biol.* **2001**, *311*, 1081−1090.
(27) Desjarlais, J. R.; Clarke, N. D. *Curr. Opin. Struct. Biol.* **1998**, *8*, 471−475.
(28) Street, A. G.; Mayo, S. L. *Structure Fold. Des.* **1999**, *7*, R105−109.
(29) Huang, S. S.; Gibney, B. R.; Stayrook, S. E.; Dutton, P. L.; Lewis, M. *J. Mol. Biol.* **2003**, *326*, 1219−1225.
(30) Skalicky, J. J.; Bieber, R. J.; Gibney, B. R.; Rabanal, F.; Dutton, P. L.; Wand, A. J. *J. Biomol. NMR* **1998**, *11*, 227−228.
(31) Huang, S. S.; Koder, R. L.; Lewis, M.; Wand, A. J.; Dutton, P. L. *PNAS* **2004**, *101*, 5536−5541.
(32) Iwata, S.; Lee, J. W.; Okada, K.; Lee, J. K.; Iwata, M.; Rasmussen, B.; Link, T. A.; Ramaswamy, S.; Jap, B. K. *Science* **1998**, *281*, 64−71.
(33) Xia, D.; Yu, C. A.; Kim, H.; Xia, J. Z.; Kachurin, A. M.; Zhang, L.; Yu, L.; Deisenhofer, J. *Science* **1997**, *277*, 60−66.
(34) Zhang, Z.; Huang, L.; Shulmeister, V. M.; Chi, Y. I.; Kim, K. K.; Hung, L. W.; Crofts, A. R.; Berry, E. A.; Kim, S. H. *Nature* **1998**, *392*, 677−684.
(35) Hunte, C.; Koepke, J.; Lange, C.; Robmanith, T.; Michel, H. *Structure* **2000**, 669−684.
(36) Salerno, J. C. *J. Biol. Chem.* **1984**, *259*, 2331−2336.
(37) Willner, I.; Heleg-Shabtai, V.; Katz, E.; Rau, H. K.; Haehnel, W. *J. Am. Chem. Soc.* **1999**, *121*, 6455−6468.
(38) Rau, H. K.; DeJonge, N.; Haehnel, W. *Proc. Natl. Acad. Sci. U.S.A.* **1998**, *95*, 11526−11531.
(39) Lombardi, A.; Summa, C. M.; Geremia, S.; Randaccio, L.; Pavone, V.; DeGrado, W. F. *Proc. Natl. Acad. Sci. U.S.A.* **2000**, *97*, 6298−6305.

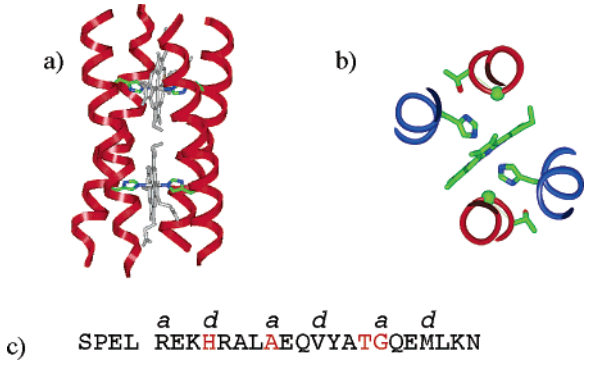

Figure 1. Model of (a) heme binding site (b) and sequence (c) of D_2-symmetric four-helix bundle. The backbone coordinates were generated by symmetry operations from a single idealized monomer, which was fit to the coordinates of cytochrome bc_1. The heme is axially coordinated by the Nϵ of two histidine side chains contained in helices 1 and 3 (blue ribbon); the orientation of each His residue is fixed by hydrogen bonding between its Nδ and a Thr residue on the neighboring helices 2 and 4 (red ribbon), as shown in part b. The critical residues (His, Ala, Thr, and Gly) are highlighted in red in the sequence (c).

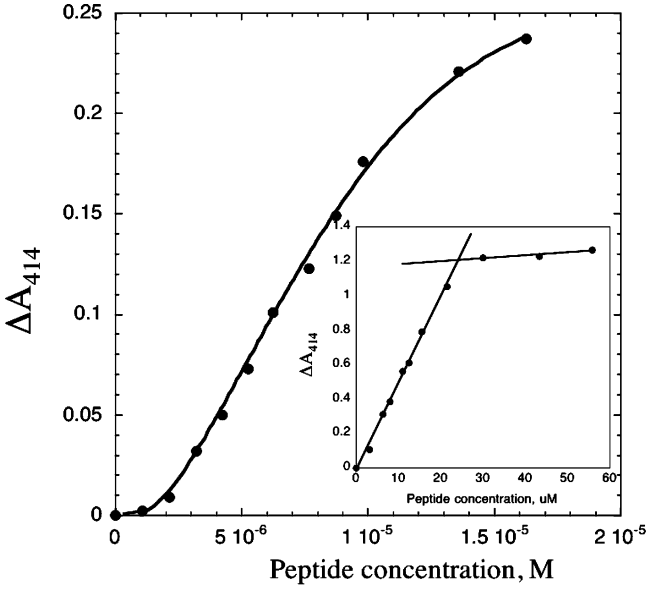

Figure 2. Heme binding isotherm for D_2-heme. The increase in absorbance at 414 nm obtained by titrating peptide into a 3.3 μM solution of hemin in phosphate buffer, pH 7.2 to final peptide concentrations in the 0 to 16 μM range is reported together with the fit obtained using a 4:2 complexation model. Insert: the same experiment conducted at a higher heme concentration (10 μM) supports the 4:2 stoichiometry.

be exposed to the aqueous environment. Thus, we introduced polar residues in these positions and designed specific polar interactions on the protein surface as described previously;[40] residues were also chosen to maximize helix propensity and sequence diversity. Because of symmetry, only the interface between the N terminal half of helix 1 and the C terminal half of the adjacent helix 1′ needed to be designed. Side chain to backbone hydrogen bonding interactions and specific charged residues were introduced at the N and C termini as capping motifs to stabilize the helical conformation. The final sequence spans 25 residues (Figure 1c).

Binding of Hemin. The D_2-heme peptide binds ferric heme, as demonstrated by the appearance of a Soret band at 415 nm (ϵ = 76 mM^{-1} cm^{-1} per site) and typical α- and β-bands at 562 and 529 nm, respectively (Figure 6a, broken line). Upon heme reduction with sodium dithionite, the optical spectrum displayed a Soret maximum at 430 nm and well-resolved α-band at 562 nm and β-band at 532 nm values (Figure 6a, solid line), typical of bis-histidine ligated *b*-type cytochromes.[14,41,42] Titration experiments, in which aliquots of protohemin IX in DMSO are added to a solution of peptide, confirmed the expected 4:2 stoichiometry. The affinity of binding was evaluated by addition of peptide, in 0.25 equivalent increments, to 3.3 μM protohemin IX solutions in PBS buffer (Figure 2). At this concentration the assembly of the complex is 90% complete within 1 h, and complete equilibration is reached overnight. The data could be analyzed according to an equilibrium in which four peptides bind two porphyrins. However, uncertainties in the fate of the free heme during long incubation times together with an estimated 5% error in the peptide concentration indicate that further studies would be necessary for an accurate evaluation of the binding constant. The titration experiment was repeated in the same conditions at higher protohemin IX concentration, namely 10 μM, to confirm the stoichiometry of binding. At this concentration, the binding isotherm shows a clear break point, corresponding to a peptide concentration of approximately 20 μM, i.e., twice that of the protoporphyrin IX. These data support a 4:2 stoichiometry for the heme/peptide complex. Typically, the dissociation constants reported in the literature for noncovalent peptide−heme complexes are in the mid-nanomolar to low micromolar range for bis-histidine ligation.[43] A direct comparison is impossible due to the different stoichiometry of the complex; however, the complex is formed at low micromolar heme concentration and is stable over several weeks. In previously designed multiheme proteins, the heme binding sites tend to have ordered affinities with the heme binding first to high-affinity sites. By contrast, the binding of the hemes appeared to occur with very strong positive cooperativity in D_2-heme; this is also consistent with evidence obtained from gel filtration and analytical sedimentation studies as described in the following sections.

Peptide Aggregation States: The aggregation state of the peptide in the apo and bound form was evaluated by gel filtration chromatography with initial loading concentrations of approximately 50 μM (Figure 3); the elution profile was monitored at 280 nm. The apo peptide elutes with a retention time consistent with a molecular weight of 3500 Da, corresponding to a monomer; in contrast, the complex obtained by treating the peptide with a stoichiometric amount of heme elutes as a species of 15 000 Da, as expected for a tetramer. The stoichiometry of the complex was confirmed to be 4:2 by determining the peptide and heme concentrations in the peak as described previously[17] (see Materials and Methods). The peak was also examined by analytical ultracentrifugation; the sedimentation curves obtained were best fit to a single species model with an apparent molecular weight of 14 800 ± 500 Da.

A substoichiometric mixture of peptide and heme, in which only 0.5 equiv of hemin was added, elutes in two fractions of approximately the same areas coeluting with the apo and bound

(40) Betz, S. F.; DeGrado, W. F. *Biochemistry* **1996**, *35*, 6955−6962.
(41) Pettigrew, G. W.; Moore, G. R. *Cytochromes c. Biological Aspects*; Springer-Verlag: Berlin, Heidelberg, New York, 1987.
(42) Yu, L.; Xu, J.-X.; Haley, P. E.; Yu, C.-A. *J. Biol. Chem.* **1987**, *262*, 1137−1143.
(43) Gibney, B. R.; Rabanal, F.; Reddy, K. S.; Dutton, P. L. *Biochemistry* **1998**, *37*, 4635−4643.

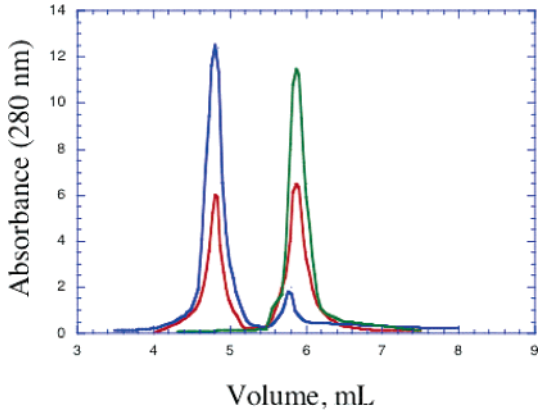

Figure 3. Gel filtration elution profile for D_2-heme in the apo state (green), in 4:2 peptide/heme stoichiometric ratio (blue), and in 1:1 peptide/heme ratio (red). The apo peptide elutes in one single peak at 6 mL, consistent with a molecular weight of 3500 Da; the 4:2 peptide/heme sample elutes in a single peak at 4.5 mL, corresponding to a MW of 15 000 Da. In contrast, the elution profile of the 1:1 peptide/heme sample shows two distinct peaks at 15 000 Da and 3500 Da, respectively.

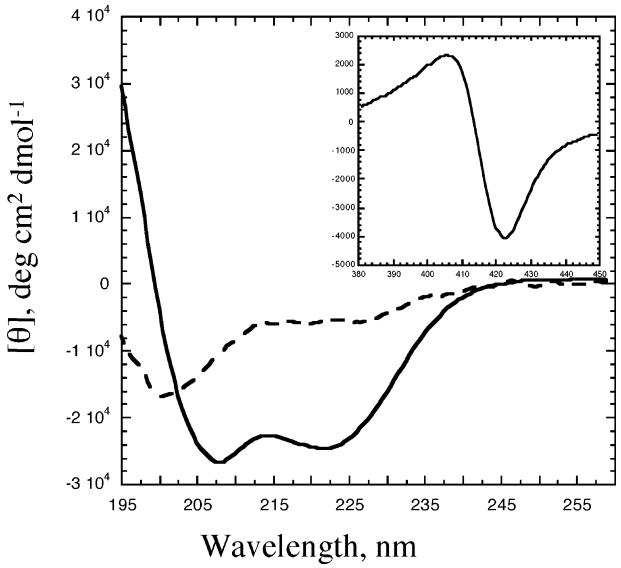

Figure 4. CD spectroscopy of D_2-heme in the apo state and in the 4:2 heme complex. The peptide is unfolded in the apo state (dotted line), while it assumes a helical conformation in the presence of heme (continuous line). The inset shows the induced dichroic signal observed in the visible part of the spectrum, corresponding to the Soret band of the heme complex.

fractions, respectively. No intermediate peaks were observed. These results indicate that the tetrameric four-helix bundle self-assembles around the hemes in a cooperative manner. No alternative assembly states such as 2:1 adducts or higher molecular weight staggered fibrils exist in solution.

CD Spectroscopy and Thermal Unfolding: The secondary structure of the peptide was determined by CD spectroscopy. In its apo form, the peptide is unfolded; upon addition of a stoichiometric quantity of heme, corresponding to one-half the total peptide concentration, the peptide folds into an α-helical structure (Figure 4), as shown by the two minima at 208 and 222 nm. Moreover, an induced dichroic signal is observed in the 400 to 450 nm range, corresponding to the absorbance range of the Soret band. As monomeric hemes in isotropic solutions show no dichroic signal,[44] the presence of this band indicates

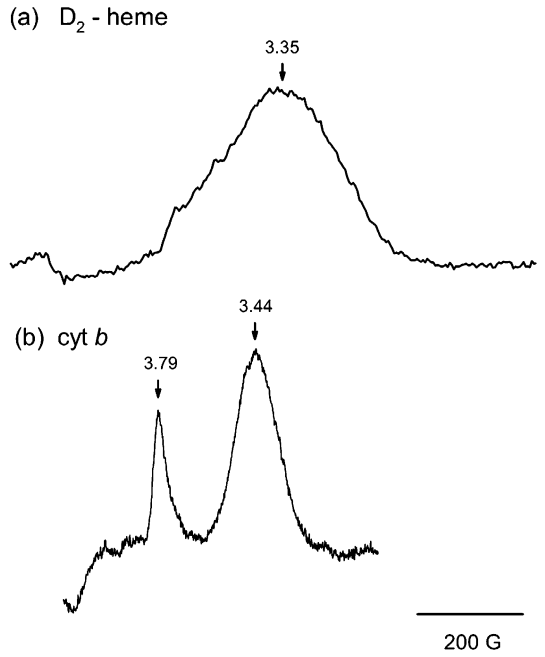

Figure 5. Comparison of the EPR spectra of the ferric heme *b* in synthetic D_2-heme peptide (a) and natural cytochrome bc_1 isolated form photosynthetic bacterium *Rba. capsulatus* (b). The insert in part a shows the complete spectral range. The samples were poised with ascorbate, leaving hemes *b* oxidized and paramagnetic. The numbers with arrows identify the *g*-values of the low-field transitions.

that the hemes are positioned in a chiral environment. The stability of the peptide was investigated by monitoring the CD signal at 222 nm at increasing temperatures. The curve obtained shows a melting point of approximately 55 °C. A more accurate analysis of the thermodynamic parameters is prevented by the apparent irreversibility of the process: at high temperatures, the heme is released in solution and is degraded. However, the addition of fresh heme to the cooled sample restores the secondary structure. These data show that the heme-bound peptide is well folded and resistant to thermal denaturation comparably with proteins of similar size.

EPR Studies: The coordination and spin state of the iron were investigated by EPR spectroscopy of the ferric heme complexes. The spectrum obtained at 20 K (Figure 5a) is dominated by low-spin Fe(III) signals, indicative of axial coordination with two strong axial ligands, as would be expected for a bis-His site. The spectrum showed no evidence for high-spin ferric heme species typically observed near $g = 6.0$, which would be expected for free or partially bound heme. The spectrum of the heme is consistent with the design and shows a highly anisotropic low-spin (HALS) spectrum[36,45−47] with low-field transition $g_{max} = 3.35$. The g_x feature was too broad to be observed but is predicted to occur at 0.7 (calculated[48] from $16 = g_{xx}^2 + g_{yy}^2 + g_{zz}^2$, which is appropriate for $(d_{yx})^2(d_{xz},d_{yz})^3$ ground states). This highly anisotropic spectrum is designated as a type I spectrum by Walker.[46,47]

An HALS spectrum has also been frequently observed in cytochrome bc_1[36] and small molecule complexes with sterically

(44) Myer, Y. P.; Pande, A. In *The Porphyrins*; Dolphin, D., Ed.; Academic Press: New York, 1978; pp 271−322.
(45) Salerno, J. C. *Biochem. Soc. Trans.* **1985**, *13*, 611−615.
(46) Walker, F. A. *Coord. Chem. Rev.* **1999**, *186*, 471−534.
(47) Benda, R.; Schunemann, V.; Trautwein, A. X.; Cai, S.; Reddy Polam, J.; Watson, C. T.; Shokhireva, T.; Walker, F. A. *J. Biol. Inorg. Chem.* **2003**, *8*, 787−801.
(48) de Vries, S.; Albracht, S. P. *Biochim. Biophys. Acta* **1979**, *546*, 334−340.

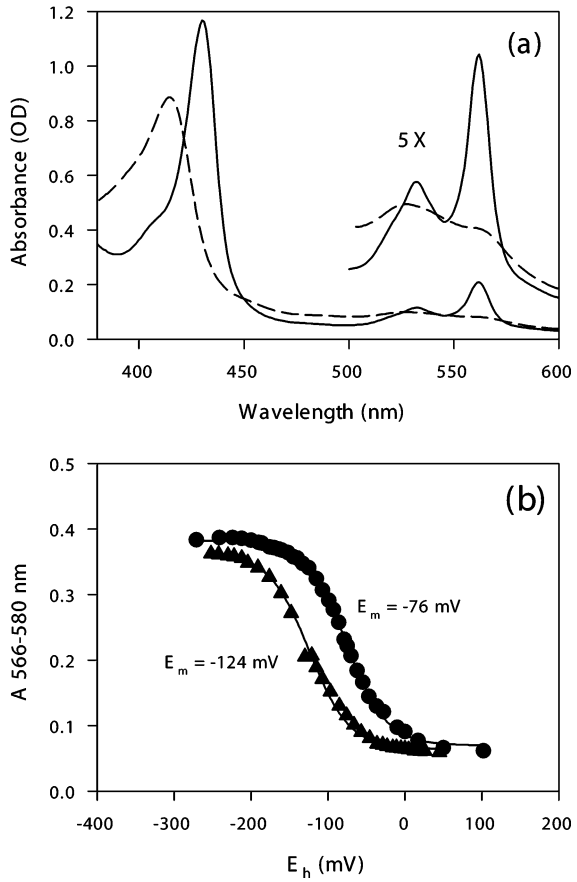

Figure 6. (a) Optical absorption spectra of D_2-heme peptide in the oxidized (broken line) and dithionite-reduced forms (solid line). (b) Potentiometric titration of D_2-heme petide. The data from reductive (circles) and oxidative (triangles) dark equilibrium redox titrations were fit to the Nernst equation for a one-electron couple, and the E_m values vs SHE are indicated.

encumbered imidazole ligands.[46] The low-field transitions of hemes *b* of cytochrome bc_1 exhibit g_{max} values greater than 3.0 (Figure 6b),[36] which has been attributed to the highly anisotropic nature of these hemes due to a roughly perpendicular conformation of the imidazole ligands of the iron of each.[49] Our synthetic peptide also exhibits a clear g_{max} transition in this region (Figure 6a) indicative of a perpendicular orientation of the ring planes of the His ligands[45,46] and fully consistent with the design, which shows approximate D_{2d} symmetry surrounding the heme site. The spectrum is also clearly different from previous unstrained bis-imidazole small molecule complexes and conformationally mobile "maquettes", which have more regular "type II" spectra (*g* values of 2.8 to 2.9, 2.3, and 1.5) consistent with a D_{2h}-symmetrical parallel orientation of the planes of the imidazole rings.

Haehnel, Lubitz, and co-workers[18,20] have designed and characterized a series of synthetic peptide models for the diheme site in cytochrome bc_1. These models show a two-component EPR spectrum, showing a mixture of type I and II spectra. Thus, while there is evidence for the perpendicular orientation of the His rings in these models, a second conformation is present with the more conventional parallel orientation. It is possible that the hydrogen bonding Thr, which is present in our models but was not included in the models of Haehnel, Lubitz et al., is important for stabilizing the perpendicular orientation of the His ring. It is also interesting to note that the g_{max} transition of our two-heme bundle is broader than that of cytochrome *b*, possibly indicative of averaging between slightly nonequivalent conformations at the two sites.

Redox Potentiometry: The redox midpoint potential of the diheme protein was determined by potentiometry at pH 8 (E_{m8})[50] following the spectral changes in the α-band (500−600 nm) that correspond to the transition between oxidized and reduced forms of the protein. Figure 6b shows that the course of oxidation−reduction followed a defined Nernst transition with an *n*-value of unity. There was, however, a pronounced hysteresis evident on the minutes time scale of the titrations. E_{m8} values of −76 and −124 mV were obtained for reductive and oxidized directions, respectively. Both E_{m8} values are significantly higher than the values of imidazole-ligated porphyrins in aqueous solution or bis-His designed peptides and proteins[16] at the same pH, suggesting that the heme-binding pocket provides significant shielding from the external aqueous phase and/or provides H-bonds or a charged environment that promotes the reduced form. On the other hand, these values are at the lower limit of the potentials of hemes *b* measured in native cytochromes bc_1,[51−53] which typically display values for heme b_H and heme b_L of +50 and −100 mV, respectively. The course of the redox titrations approximates a single transition indicating that if the two hemes do have different E_m values they are within 20−30 mV of each other, the limit of measurements in these titrations. Similarity of the E_m values of the two hemes in the designed bundle suggests that the two binding sites remain similar in the symmetrically designed protein and also that there is no significant charge interaction between the two hemes.[14,43] This is not the situation in the natural cytochrome bc_1 where the two hemes are positioned in four different helices surrounded by different residues.

The hysteresis clearly evident in the titrations can be attributed to slow equilibration between two distinct conformations, one more stable in the oxidized state, and the other favored in the reduced state. We note that the titration curve observed in the oxidative direction relaxes to the one with a potential of −124 mV observed in the reductive direction within 30 min, thus indicating that the latter is favored. The perpendicular orientation of the imidazole rings is significantly less favorable in the ferrous as opposed to ferric hemes.[46] Here, we speculate that the slow conformational change might involve a shift in the planes of the His ligands. However, a detailed study of the structure and stability of the ferrous versus the ferric complexes will be necessary to support this speculation.

NMR Spectroscopy: Natural proteins possessing a unique well-folded native state yield NMR spectra with characteristically well-dispersed chemical shifts and narrow line widths in the amide and aliphatic regions. The one-dimensional ^{1}H NMR spectrum of the heme-bound protein possesses the same distinctive features (data not shown), indicating that the protein exists in solution in a well-folded single conformation. In sharp

(49) Walker, F. A. *Chem. Rev.* **2004**, *104*, 589−616.
(50) Dutton, P. L. *Methods Enzymol.* **1978**, *54*, 411−435.
(51) de Vries, S.; Albracht, S. P.; Leeuwerik, F. J. *Biochim. Biophys. Acta* **1979**, *546*, 316−333.
(52) Von Jagow, G.; Schagger, H.; Engel, W. D.; Hachenberg, H.; Kolb, H. J. In *Energy Conservation in Biological Membranes*; Schafer, G., Klingenberg, M., Eds.: Berlin, 1978; p 43.
(53) Moser, C. C.; Giangiacomo, K. M.; Matsuura, K.; de Vries, S.; Dutton, P. L. *Methods Enzymol.* **1986**, *126*, 293.

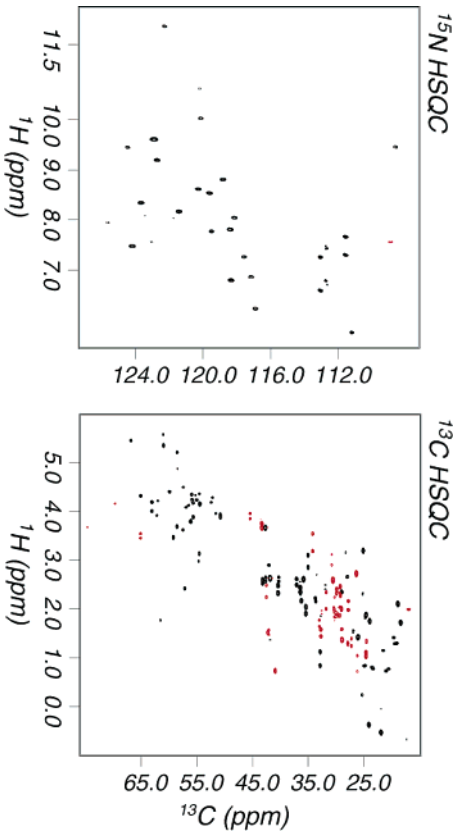

Figure 7. ^{15}N HSQC (top) and natural abundance ^{13}C HSQC (bottom: in black, positive intensity peaks; in red, negative intensity peaks) of the ferric heme complex; the well-resolved resonances are indicative of a unique conformation.

contrast, the broad spectrum of the apo protein is typical of unfolded peptides.

To simplify the assignment of the resonances, we substituted protohemin IX for its symmetric analogue, protohemin III. Samples reconstituted with protohemin IX show multiple sets of signals with various degrees of overlap, due to the different orientations that each of the two prosthetic groups could assume in the complex. In contrast, these signals collapse into one single set when the sample is reconstituted with protohemin III.

The natural abundance ^{13}C HSQC spectrum, reported in Figure 7, shows well resolved, sharp resonances in both dimensions in the methyl and methylene areas, indicating a unique chemical environment. Examination of the ^{15}N HSQC spectrum shows that the backbone amide resonances are also well dispersed. We conclude that D_2-heme displays spectral properties comparable with those of native proteins and is amenable to structural studies by solution NMR.

Conclusions

The use of a mathematical model to generate a backbone model closely resembling the central four-helix bundle of cytochrome bc_1 has expedited the design of a tetrameric heme-binding protein. At the level of the backbone structure, the central four-helix bundle of cytochrome bc_1 can be described by a D_2-symmetrical model with a single helix in the asymmetric unit. However, as discussed by Haehnel and Lubitz,[18,20] the symmetry is lowered to C_2 if one considers the functional side chains, which define a heme-ligating and a heme-blocking helix. Nevertheless, the good fit of the D_2 model to the experimental structure suggested that it would be possible to design a fully symmetrical peptide. As a result of the D_2-symmetrical restraint, the resulting protein has a novel topology, in which the heme−heme distance is 6 Å shorter than that in cytochrome bc_1.

The D_2-heme assembly displays the hallmarks of uniquely folded native proteins and will provide a framework for investigating second-shell ligand effects on the properties of the heme. Also, the parameters describing the backbone can be varied in successive iterations and coupled with automated sequence selection algorithms to generate entirely novel structures optimized to bind non-natural cofactors.

Materials and Methods

Design. The backbone of the peptide was generated as described previously:[26] briefly, we extended the Crick parametrization for a coiled coil model to include the antiparallel orientation of the helices. The hemes were positioned with their heme iron atoms directly on the central axis of the coiled coil and its propionate groups pointing out of the ends of the bundle, as in cytochrome bc_1. One His ligand was introduced into each helix with mean side chain torsional angles taken from the structure of cytochrome bc_1. The conserved Gly and Thr residues were next introduced, which resulted in a good fit between the heme and the helical bundle, as well as an interhelical hydrogen bond between the Thr and His side chains. These keystone interactions uniquely define the geometry of the bundle. The remaining space within the interior of the bundle was so highly constrained that it was possible to choose the remaining hydrophobic residues by visual inspection. The exterior residues were designed to optimize the desired geometry and destabilize alternatives.[54] The final model was refined by energy minimization using esff in the Discover3 module.

Materials. Fmoc-protected amino acids (Fmoc: 9-fluorenylmethoxycarbonyl), PAL resin (PAL: 5[4-(aminomethyl)-3,5-bis(methoxy)-phenoxy]valeric acid), HOBt (*N*-hydroxybenzotriazole), and HBTU (2-(1*H*-benzotriazole-1-yl)-1,1,3,3-tetramethyluroniumhexafluorophosphate) were purchased from NovaBiochem. All solvents and chemicals used in the peptide synthesis and purification were of the highest available grade and were used without further purification. Protohemin IX was purchased from Porphyrin Products.

Synthesis. The peptides were synthesized with standard solid-phase procedures on an ABI 433 synthesizer (PE Applied Biosystems) equipped with a UV detector to monitor Fmoc deprotection (Alltech) and purified by reverse-phase HPLC on a semipreparative C_4 column (Vydac). All peptides were acetylated at the amino terminus. The peptides were determined to be at least 95% pure by analytical HPLC; MALDI mass spectrometry confirmed the expected molecular weight and purity. The synthetic peptide was used for all the experiments described here, except for the NMR experiments. Protoporphyrin-III dimethyl ester (6,7-bis[2-(methoxycarbonyl)ethyl]-1,4,5,6-tetramethyl-2,3-divinyl porphyrin) was synthesized from monopyrroles;[55] iron insertion and ester hydrolysis were performed as previously described.[56]

Determination of Aggregation State. Gel filtration elution profiles were obtained on a Superdex 75 column on an FPLC system (Amhersham Pharmacia Biosystems); typically, 100 μL of approximately 0.5 mM stock solution of peptide were loaded and eluted with 0.01 M sodium phosphate, pH 7.2, containing 0.2 M NaCl at 0.5 mL/min. To determine the stoichiometry of heme binding, peptide concentrations in the fractions collected for the 4.5 mL peak (approximately 15,000 Da) were determined by HPLC, integrating the UV−vis monitored elution peak of the peptide on a C_{18} reverse-phase

(54) Summa, C. M.; Rosenblatt, M. M.; Hong, J. K.; Lear, J. D.; DeGrado, W. F. *J. Mol. Biol.* **2002**, *321*, 923−938.
(55) Smith, K. M.; Parish, D. W.; Inouye, W. S. *J. Org. Chem.* **1986**, *51*, 666−671.
(56) Smith, K. M.; Fujinari, E. M.; Langty, K. C.; Parish, D. W.; Tabba, H. D. *J. Am. Chem. Soc.* **1983**, *105*, 6638−6646.

column; known concentrations of pure peptide were used to calibrate the column. Heme concentrations in the same fractions were determined by the pyridine-hemochrome method.[57]

Sedimentation equilibrium analysis was performed using a Beckman XLI analytical ultracentrifuge. The complex was assembled in PBS buffer and purified by gel filtration on a P10 column prior to the experiment. Initial peptide concentrations were 0.1 mM in 0.01 M sodium phosphate, pH 7.2, containing 0.05 M NaCl. The samples were centrifuged at 35 000, 40 000, and 45 000 rpm; equilibrium was determined when successive interference radial scans at the same speed were indistinguishable. Interference fringe data and absorbance data at 280 and 414 nm were collected. Partial specific volumes were determined by the residue-weight average method of Cohn and Edsal. Solution densities were estimated using solute concentration-dependent density tables in the CRC Handbook of Chemistry and Physics. Curve fitting to the data was done using Igor Pro (WaveMetrics, Inc.) with procedures adapted from Brooks et al..[58]

Redox Titrations. Chemical oxidation−reduction midpoint potential titrations of complexes purified by gel filtration were performed as described.[50] The titrations were performed in 50 mM Tris-HCl (pH 8.0) containing 100 mM NaCl and redox mediators: 2,3,5,6-tetramethyl-1,4-phenylenediamine, phenazine ethosulfate, phenazine methosulfate, duroquinone, pyocyanine, indigotrisulfonate, 2-hydroxy-1,4-naphthoquinone, anthraquinone-2,6-disulfonate, anthraquinone-2-sulfonate, and benzyl viologen at concentrations of 15−30 μM. The concentration of the peptide was 2 μM. The optical changes (in the region 500−600 nm) that accompanied redox potential change were recorded on a Perkin-Elmer UV/vis spectrophotometer (Lambda 20) fitted with an anaerobic redox cuvette. At each solution redox potential, the sample was allowed to equilibrate for approximately 5 min. The E_m values were determined by fitting the data to a single $n = 1$ Nernst expression.

EPR Measurements. EPR spectra of the synthetic D_2-heme peptide (purified by gel filtration) and native cytochrome bc_1 (purified form from photosynthetic bacterium *Rhodobacter capsulatus*[59]) were obtained on a Brucker ESP300E spectrometer with temperature control maintained by an Oxford ESR 900 continuous-flow liquid helium cryostat interfaced with an Oxford ITC4 temperature controller. The frequency was measured by a Hewlett-Packard 5350B frequency counter. The EPR parameters were as follows: sample temperature, 20 K; microwave frequency, 9.447 GHz; microwave power, 2 mW; modulation frequency, 100 kHz; modulation amplitude, 20.0 G; time constant, 164 ms.

CD Measurements. CD spectroscopy was carried out at 25 °C using a CD spectrometer (Aviv Associates); temperature-dependent denaturation experiments were performed recording the ellipticity at 222 nm versus temperature (conditions: 0.01 M sodium phosphate buffer pH 7.0, NaCl 0.1 M; peptide concentration was 5 μM).

Binding Affinity. The binding affinity of the peptide for heme was evaluated by titrating increasing amounts of peptide into a solution containing 3.3 μM heme in PBS buffer. Samples containing peptide concentrations in the 0 to 16 μM range were equilibrated overnight. Complex formation was monitored by measuring the height of the Soret band at 414 nm. The experiment was repeated at a higher heme concentration (10 μM).

Protein Expression and Purification. The recombinant D_2-heme peptide used in the NMR experiments was prepared by overexpressing the corresponding synthetic gene in *E. coli* BL21(DE3) cells. The two complementary strands coding for the peptide, codon optimized for expression in *E. coli* and including BamHI and HindIII restriction sites, were annealed, phosphorylated, and digested previous to insertion into a modified pET-32b vector (Novagen) using standard methods. The vector[60] contains the IPTG-inducible T7 promoter and thioredoxin fusion protein. The chimeric protein comprises a thioredoxin fusion partner and a His-tag sequence N terminal to the desired peptide. The final peptide sequence includes an N-terminal Gly retained after digestion of the thioredoxin-peptide fusion protein with thrombin, as a result of the overlapping of the BamHI restriction site with the thrombin cleavage site. A suboptimal GGA codon for Gly was utilized because it is part of the BamHI restriction site. The BL21(DE3) cells were grown to an OD of 0.6 prior to induction with 1 mM IPTG; after 4 h, the cells were harvested, lysed in 6 M guanidinium chloride, and clarified by centrifugation. The fusion protein was purified using a Ni-NTA His-bind column (Novagen) and dialyzed twice for 2 h to exchange out the imidazole. Following thrombin cleavage, the peptide was isolated by a second Ni-NTA His-bind column, lyophilized, and purified by reverse-phase HPLC using a C_4 column (Vydac). For overexpression of the $^{15}N-^{13}C$-labeled protein, cells were initially grown on rich media, then harvested, and transferred to minimal media containing $^{15}NH_4Cl$ (Isotech) and $^{13}C_6$ glucose as sole sources of N and C prior to induction.[61]

NMR Spectroscopy. Nuclear magnetic resonance spectra were recorded on Varian INOVA spectrometers operating at 600 MHz (^1H), using a standard Varian 5 mm triple-resonance probe with three-axis pulse field gradients. Proton chemical shifts were referenced to an external standard of DSS in D_2O; ^{13}C and ^{15}N chemical shifts were referenced indirectly using the consensus X_i ratios of gyromagnetic ratios, 0.101 329 118 and 0.251 449 528 for $^{15}N/^1H$ and $^{13}C/^1H$, respectively.[62] For all experiments, the ^1H carrier frequency was set to the water resonance. ^{13}C, ^{15}N-enriched de novo designed heme proteins were successfully prepared by expression during growth on minimal media. The protein samples were dissolved in a solution of 95% H_2O, 5% D_2O, 50 mM potassium phosphate, pH 6.0. The protein concentrations of both ^{13}C- and ^{15}N-labeled samples were 1 mM. The latter sample (300 μL) was prepared in a Shigemi Microcell NMR tube (Shigemi, Inc.) $^1H-^{15}N$ HSQC[63,64] and $^1H-^{13}C$ HSQC[61] (Heteronuclear Single Quantum Coherence) experiments were collected at 293 K.

Acknowledgment. This work was supported by NIH Grants GM54616 to W.F.D, GM 48130 to P.L.D., HL-22252 to K.M.S., and GM 35940 to A.J.W. and by the NSF MRSEC award DMR00-79909 to A.J.W. G.G. also thanks Andrew L. Lee, Steve J. Lahr, and Enrico Surace for advice on the cloning and expression protocols and Ronald L. Koder for helpful discussions.

JA039935G

(57) Berry, E. A.; Trumpower, B. L. *Anal. Biochem.* **1987**, *161*, 1−15.
(58) Brooks, I. S.; Soneson, K. K.; Hensley, P. *Biophys. J.* **1993**, *64*, 244.
(59) Valkova-Valchanova, M. B.; Saribas, A. S.; Gibney, B. R.; Dutton, P. L.; Daldal, F. *Biochemistry* **1998**, *37*, 16242−16251.
(60) Lee, A. L.; Kinnear, S. A.; Wand, A. J. *Nat. Struct. Biol.* **2000**, *7*, 72−77.
(61) Marley, J.; Lu, M.; Bracken, C. *J. Biomol. NMR* **2001**, *20*, 71−75.
(62) Wishart, D. S.; Bigam, C. G.; Yao, J.; Abildgaard, F.; Dyson, H. J.; Oldfield, E.; Markley, J. L.; Sykes, B. D. *J. Biomol. NMR* **1995**, *6*, 135−140.
(63) Kay, L. E.; Keifer, P.; Saarinen, T. *J. Am. Chem. Soc.* **1992**, *114*, 10663−10665.
(64) Zhang, O. W.; Kay, L. E.; Olivier, J. P.; Forman-Kay, J. D. *J. Biomol. NMR* **1994**, *4*, 845−858.